Zero : Jurnal Sains, Matematika, dan Terapan
E-ISSN : 2580-5754; P-ISSN : 2580-569X
Volume 10, Number 2, 2026
DOI: 10.30829/zero.v10i2.31303
Page: 805-817

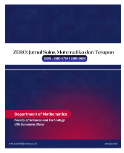

Pricing European Call Options on LQ45 Stocks under Transaction Costs: A Barles-Soner-GARCH Approach

[1]**Nasya Widiani**
Mathematics Department, Universitas Negeri Surabaya, Kediri, 64157, Indonesia

[2]**Rudianto Artiono**
Mathematics Department, Universitas Negeri Surabaya, Surabaya, 60241, Indonesia

Article Info

Article history:

Accepted: 23 August 2026

Keywords:

Barles-Soner;
European options;
GARCH;
LQ45;
Transaction costs.

ABSTRACT

This study prices European call options on 27 constituent-verified LQ45 stocks (February 2022-December 2025) with a Barles-Soner-GARCH framework benchmarked against Black-Scholes-GARCH. The 27 names are the survivors of 72 tickers screened against every official constituent evaluation in the window, so the panel is by construction the exchange's most persistently liquid segment and the figures below are conservative for that reason. Stock-level GARCH (1,1) forecasts supply the volatility inputs for 1,620 scenarios spanning moneyness, maturity and proportional transaction costs. At zero cost the finite-difference solver reproduces the analytical benchmark to a 0.10% mean relative error, and grid refinement confirms this is not mesh-specific. Because the nonlinear correction is non-negative by construction, a positive premium is structural rather than an empirical finding, so the informative quantities are its magnitude and cross-sectional pattern. The premium rises from 3.02% of spot at a cost of 0.005 to 7.51% at 0.020, but decomposing observable Indonesian trading costs places the representative one-way cost between 0.00250 and 0.00862, which puts the practically relevant premium nearer 1.51%-4.39% of spot and identifies 0.020 as a stress scenario. The premium concentrates in longer-maturity, high-gamma contracts on high-volatility stocks.

Corresponding Author

Rudianto Artiono,
Mathematics Department
Universitas Negeri Surabaya, Surabaya, Indonesia
Email: rudiantoartiono@unesa.ac.id

1. INTRODUCTION

The volatility spikes of the 2008 financial crisis and the 2020 COVID-19 pandemic showed that the constant-volatility assumption of conventional option pricing misrepresents actual markets. Indonesian LQ45 volatility likewise moves in clusters and carries issuer-specific uncertainty [1]. The Black-Scholes model derives closed-form European prices from geometric Brownian motion, constant volatility, a constant risk-free rate and a frictionless market [2], [3]; useful as a benchmark, those assumptions understate prices once hedging is repeated in an imperfect market [4], [5], [6]. The direction of that bias is not accidental: a writer rebalancing a delta hedge pays the round-trip cost at every adjustment, and the number of adjustments grows with the curvature of the position, so replicating a convex payoff costs strictly more than its frictionless value. Any correction pricing that cost must raise the premium, which is why the effect below is structural in sign and the empirical question is its size. The stake is practical: hedges on LQ45 names are executed against commissions, levies and spreads, so a frictionless benchmark leaves the unhedged residual with the writer.

Two strands address these limits. GARCH models supply dynamic volatility inputs: the conditional GARCH framework of Escobar-Anel et al. [7], the volatility-derivative extension of Oh and Park [8] and the realized-GARCH scheme of Fang and Han [9], with [10] and [11] using option data to sharpen affine-GARCH estimation, [12] and [13] discriminating among specifications by implied-volatility accuracy, [14] comparing GARCH against autoregressive stochastic volatility, and [15] and [16] extending to currency and cryptocurrency underlyings. These improve volatility estimates but leave proportional transaction costs out of the pricing equation. Separately, the nonlinear Barles-Soner equation [17] and Leland's replication-cost argument [18] correct prices for hedging frictions through a risk-aversion-based volatility adjustment. Noor and Artiono [19] and Taufik and Artiono [20] apply Barles-Soner to European options with transaction costs, but both illustrate a single underlying with no empirical LQ45 panel; wider nonlinear work [21], [22], [23], [24], [25], [26], [27] stays outside the Indonesian equity setting. Evidence on the Indonesian premium is consequently limited.

Three gaps remain. Transaction-cost pricing has not been applied to constituent-verified multi-stock LQ45 samples, although the index is the exchange's official set of high-liquidity large caps; Indonesian empirical work has addressed index volatility and return dynamics rather than nonlinear pricing with proportional costs [1]; and while finite differences are established as stable for such equations [28], [29], [30], implementations are rarely combined with GARCH volatility from market data. This study therefore prices European calls on constituent-verified LQ45 stocks with a Barles-Soner-GARCH framework against a Black-Scholes-GARCH benchmark, quantifying the premium across moneyness and maturity. The contribution is empirical scope and verification, not theoretical novelty: the equation, the sign of its correction and the GARCH-input idea are established, and [19] and [20] already price European options under the same model. What is added is a constituent-verified 27-stock panel, stock-level GARCH(1,1) volatility fed to both models, a solver validated at the zero-cost boundary and under grid refinement, and a 1,620-scenario grid calibrated against measured Indonesian trading costs.

2. RESEARCH METHOD

This is a computational study in financial mathematics. European call prices on verified LQ45 stocks are obtained by combining GARCH volatility estimation, the Black-Scholes benchmark and the Barles-Soner nonlinear transaction cost model, so that price changes can be attributed to relaxing the constant-volatility and zero-cost assumptions. Figure 1 shows the flow from constituent verification through return processing, volatility estimation, pricing, solver validation and model comparison.

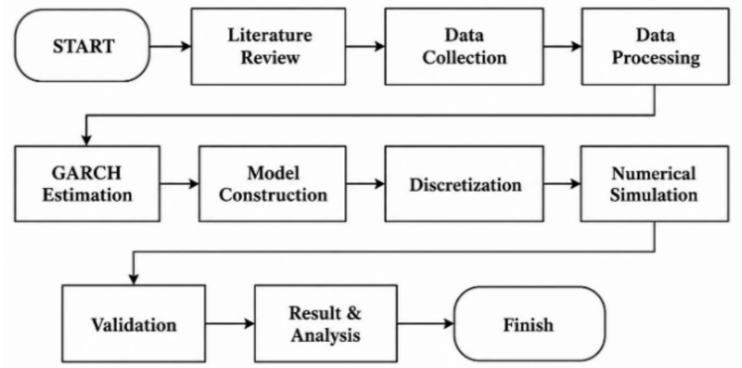

Figure 1. Flowchart

2.1 Research Data and Objects

The research objects are stocks continuously listed as LQ45 constituents across the observation period. Two counts govern the sampling and are distinct: seventeen official Indonesia Stock Exchange announcement and evaluation documents were consulted, more than the number of semi-annual reviews because major evaluations, minor evaluations and fast-entry announcements are all included, and seventy-two distinct tickers appear somewhere in those documents, of which twenty-seven appear in all seventeen. Price data are complete when a stock has 937 observations on the common trading calendar with no missing values.

Corrected daily closing prices for 2 February 2022 to 30 December 2025 came from Yahoo Finance using .JK tickers, with constituent status verified against the official documents. Corrected prices adjust for corporate actions. Of the 72 tickers in those documents, 27 appear in all of them with complete data: ADRO, AMRT, ANTM, ASII, BBCA, BBNI, BBRI, BBTN, BMRI, BRPT, CPIN, EXCL, ICBP, INCO, INDF, INKP, ITMG, KLBF, MDKA, MEDC, PGAS, PTBA, SMGR, TLKM, TOWR, UNTR and UNVR. That filter has a bias worth stating: the retained names stayed in the index throughout, so the panel is by construction the exchange's most persistently liquid segment. Estimated spreads therefore understate the broader market, and the frictionless benchmark is more defensible here than for smaller caps, so the premiums below are conservative. Two features bound the scope. Yahoo Finance adjustments are not independently validated against exchange records, so an internal screen was run for the failure mode that matters: an unadjusted split appears as an isolated daily log return near $\ln\left(\frac{1}{2}\right)$, $\ln\left(\frac{1}{4}\right)$, $\ln\left(\frac{1}{5}\right)$ or $\ln\left(\frac{1}{10}\right)$. No return within 0.05 of those values occurs in any series, the largest absolute daily log return is 0.283 for ADRO, inside the auto-rejection limits, and no missing or non-positive prices remain, so gross adjustment failures can be excluded even though residual error cannot. Second, no traded option quotes are used: every value is a model output on verified equity inputs, so the claims concern the magnitude of the correction rather than agreement with observed premiums. The cost parameter is calibrated to measured Indonesian levels below.

Let S_t denote the corrected closing price of a stock on the t- th trading day. The daily logarithmic return is calculated as:

$$r_t = \ln\left(\frac{S_t}{S_{t-1}}\right) \tag{1}$$

where S_t and S_{t-1} are the corrected closing prices on trading days t and $t-1$. The return series are then used for descriptive statistics, preliminary statistical tests, and GARCH volatility estimation.

2.2 Preliminary Statistical Tests

Each return series is screened in three steps. Descriptive statistics are computed per stock, covering observations, mean, standard deviation, minimum, maximum, skewness and kurtosis. Stationarity is tested with the Augmented Dickey-Fuller test, its lag chosen automatically by the Akaike criterion, a p-value below 0.05 rejecting the unit root at the 5% level, since GARCH models are conventionally estimated on stationary returns. Conditional heteroscedasticity is tested with ARCH-LM at lag 12, rejection at the 5% level justifying the GARCH family, and the same test is reapplied to the standardized residuals afterwards to check that the fitted model removes the effect.

2.3 GARCH Volatility Estimation

The volatility input is a GARCH(1,1) forecast, used because returns show volatility clustering that makes constant volatility too restrictive [12], [7], [8], and because GARCH models are established for LQ45 dynamics [1]. The baseline is GARCH(1,1) with normal innovations, and the reason is not goodness of fit. The evidence points the other way: several stocks show marked excess kurtosis and non-zero skewness in Table 4, and the Akaike criterion prefers Student-t innovations for all 27 stocks, as reported below. The normal law is retained because it is the conventional reference for the Black-Scholes-GARCH comparator and for the prior Barles-Soner results on Indonesian data [19], [20], and because it yields the smaller correction, making every headline premium the conservative one. Comparability does not settle the choice, since a single Student-t law applied identically would serve as well. The heavier-tailed specification is therefore a reported result rather than a caveat: estimated on the full panel, carried through the whole grid and summarised in Table 8, it leaves the conclusions intact.

The return equation is defined as:

$$r_t = \mu + \varepsilon_t \tag{2}$$

where μ is the conditional mean and ε_t is the innovation component. Innovation is written as:

$$\varepsilon_t = \sigma_t z_t \tag{3}$$

where σ_t is the conditional standard deviation and z_t is the standardized error. The GARCH(1,1) variance equation is given by:

$$\sigma_t^2 = \omega + \alpha_1 \varepsilon_{t-1}^2 + \beta_1 \sigma_{t-1}^2 \tag{4}$$

where $\omega > 0$, $\alpha_1 \geq 0$, and $\beta_1 \geq 0$. The parameter α_1 measures the short-term response of volatility to the previous period's shock, while β_1 measures the persistence of past volatility. The parameters $\mu, \omega,\ \alpha_1$, and β_1 are estimated by maximum likelihood, separately for each series, with a constant conditional mean and a normally distributed standardized innovation. That assumption understates tail risk for the heaviest-tailed series: ADRO and PTBA show sample kurtosis of 15.96 and 12.76 in Table 4, against the Gaussian value of 3.

The volatility input is the one-step-ahead conditional variance forecast produced by the fitted model at the final observation of each series, not the long-run unconditional variance implied by the parameter estimates. It is converted to annual volatility using:

$$\sigma_{ann} = \sigma_{daily}\sqrt{252} \tag{5}$$

Here 252 is the number of trading days per year, matching the solver's 252 time steps so annualisation and time discretisation agree. The resulting stock-level annual volatility is the input to both models.

2.4 Black-Scholes Benchmark Model

The Black-Scholes model serves as the frictionless benchmark because it gives closed-form European prices. Let S_0 be the current stock price, K be the strike price, T be the time to maturity, r be the risk-free interest rate, and σ_{ann} be the annual GARCH volatility. The European call price is:

$$C_{BS} = S_0 N(d_1) - Ke^{-rt} N(d_2) \tag{6}$$

where

$$d_1 = \frac{\ln\left(\frac{S_0}{K}\right)+\left(r+\frac{1}{2}\sigma_{ann}^2\right)T}{\sigma_{ann}\sqrt{T}}, \tag{7}$$

$$d_2 = d_1 - \sigma_{ann}\sqrt{T} \tag{8}$$

In this equation, $N(\cdot)$ represents the standard normal cumulative distribution function. The analysis is restricted to call options because their payoff is fixed and directly comparable across stocks, strikes, maturities and cost scenarios; puts follow by put-call parity and are left aside to keep the comparison focused.

2.5 The Barles-Soner Nonlinear Transaction Cost Model

Barles-Soner extends Black-Scholes by carrying transaction costs into a nonlinear volatility function, since the frictionless assumption ignores the cost of rebalancing a hedge. Nonlinear models of this kind yield higher and more conservative values than frictionless counterparts [19], [1], [20].

The nonlinear Barles-Soner equation for a European call option is written as:

$$\frac{\partial V}{\partial t} + \frac{1}{2}\sigma^2(S,t,V_{ss})S^2\frac{\partial^2 V}{\partial S^2} + rS\frac{\partial V}{\partial S} - rV = 0 \tag{9}$$

where $V(S,t)$ is the option value, S the underlying stock price, t the time period, r the risk-free interest rate, and V_{ss} the second derivative with respect to the stock price. Volatility here is not constant but depends on option gamma. The local variance at spatial node S_i and the time-to-maturity variable τ are expressed as:

$$\sigma_i^2(\tau) = \sigma_0^2\left[1 + \Psi\left(e^{r\tau}a^2S_i^2\Delta_i(u)\right)\right] \tag{10}$$

where σ_0 is the GARCH annual volatility, $\Delta_i(u)$ is the finite difference approximation for option γ at node S_i and a^2 represents the transaction cost intensity multiplied by the risk aversion multiplier. In a computational implementation, a^2 is defined as:

$$a^2 = \lambda^2 R \tag{11}$$

where λ represents the proportional transaction cost scenario and R is the risk aversion multiplier. This study sets $R = 1$ as the baseline normalization so that nonlinear price changes are driven by the transaction cost scenario. Different R values represent different degrees of risk aversion. Because the cost intensity enters the correction as a squared cost scaled by that multiplier, the premium magnitudes depend on it, and one is a normalisation rather than a market estimate. Its influence is therefore tested rather than assumed: the full grid is recomputed at multipliers of 0.5, 1, 2 and 5, reported in Table 9.

The function $\Psi(\cdot)$ is the Barles-Soner volatility correction function. It is evaluated numerically from the ordinary differential equation:

$$\Psi'(x) = \frac{\Psi(x)+1}{2\sqrt{x\Psi(x)-x}}, \qquad \Psi(0) = 0 \tag{12}$$

Because Equation (12) is singular around zero, the numerical implementation for small positive values $x_0 = 10^{-8}$ uses an asymptotic approximation:

$$\Psi(x_o) = \left(\frac{3}{2}\right)^{\frac{2}{3}} x_0^{\frac{1}{3}} \tag{13}$$

The correction function is computed on the search grid and interpolated during the finite-difference iterations. To prevent explosive values it is capped at 5, a numerical stabilisation device rather than a calibrated parameter, so its incidence is measured rather than assumed away. Across the 1,296 positive-cost scenarios the cap binds at some node in 1,132, yet affects only 1.73% of interior node-time pairs on average, rising from 0.03% at a cost of 0.005 to 4.14% at 0.020 and reaching 48.6% in the most extreme cell. Re-solving with the cap at 100 leaves the mean premium at 0.005 unchanged to within 0.01 percentage points but lifts it from 7.51% to 8.31% of spot at 0.020, so premiums at the highest cost are mildly cap-limited and conservative, while those at the calibrated costs are unaffected.

2.6 Numerical Solution

The Barles-Soner equation is solved using a finite difference scheme. The terminal payoff of a European call option is:

$$V(S,T) = max(S-K,0) \tag{14}$$

where K is the strike price. The boundary conditions are defined as:

$$V(0,t) = 0, V(S_{max},t) = S_{max} - Ke^{-r(T-t)} \tag{15}$$

To solve the problem backward from maturity, the time-to-maturity variables $\tau = T - t$ and $u(S,\tau) = V(S,t)$ are introduced. The spatial domain $[0, S_{max}]$ is discretized into N stock price nodes with a distance of ΔS. The first and second derivatives are approximated using central differences:

$$\frac{\partial u}{\partial S}(S_i,\tau) \approx \frac{u_{i+1}(\tau)-u_{i-1}(\tau)}{2\Delta S} \tag{16}$$

and

$$\frac{\partial^2 u}{\partial S^2}(S_i, \tau) \approx \frac{u_{i-1}(\tau) - 2u_i(\tau) + u_{i+1}(\tau)}{(\Delta S)^2} \quad (17)$$

At each step the gamma of Equation (17) updates the nonlinear volatility of Equation (10), and the resulting tridiagonal system is solved semi-implicitly with frozen γ, which keeps the scheme stable while retaining the transaction cost adjustment.

Table 1 lists the numerical parameters. The upper price limit is four times the larger of spot and strike, keeping the right-hand boundary far from the valuation point. The risk-free rate, r=0.060, is a controlled baseline taken from the 6.00% BI-Rate of the Bank Indonesia Board meeting of 17-18 December 2024, held constant so that price differences reflect volatility and costs. Since the policy rate in fact moved over the observation window, this is a controlled-scenario device rather than a claim of realism.

Neither that rate nor the risk-aversion normalisation is left untested. Re-solving the grid at 4, 5, 6, 7 and 8 percent moves the mean premium relative to spot by at most 0.13 percentage points at a cost of 0.020, from 7.57% to 7.44%, and by 0.06 points at 0.005, with the leading stocks and the dominant cell unchanged; the premium falls mildly in the rate because a higher rate lifts the frictionless benchmark faster than the correction. The rate is thus an order of magnitude less influential than the risk-aversion multiplier, which is why the latter is carried into the main grid and swept in Table 9.

Table 1. Numerical Parameters of the Barles-Soner-GARCH solver

Parameter	Symbol	Value
Spatial nodes	N	180
Time steps per year	n_t	252
Upper limit multiplier	q	$4\max(S_0, K)$
Risk aversion multiplier	R	1.000
Maximum correction	C_{max}	5.000
Risk-free rate	r	0.060

2.7 Scenario Design and Model Comparison

Pricing experiments run over controlled scenarios of moneyness, maturity and proportional cost. Moneyness is represented by $\frac{K}{S_0}$, with values below one in-the-money, one at-the-money and above one out-of-the-money. Table 2 gives the design.

Table 2. Option Pricing Computation Scenario Design

Scenario Component	Symbol	Value
Moneyness	$\frac{K}{S_0}$	0.90, 1.00, 1.10
Maturity	T	$\frac{1}{12}$, $\frac{1}{4}$, $\frac{1}{2}$, 1 year
Transaction Cost	λ	0.000, 0.005, 0.010, 0.015, 0.020
Option Type	C_E	European Call Option

Moneyness values 0.90, 1.00, and 1.10 are the in-the-money, at-the-money and out-of-the-money levels near spot. Maturities $\frac{1}{12}$, $\frac{1}{4}$, $\frac{1}{2}$, and 1 year cover monthly to annual horizons. Costs from 0.000 to 0.020 form a controlled friction range, zero serving as the Black-Scholes validation limit.

For each of the 27 verified LQ45 stocks, the last corrected closing price was used as the spot price S_0. The strike price was determined by $K = mS_0$, where m is the moneyness level. Each stock is evaluated over 60 scenarios from three moneyness levels, four maturities and five cost levels, so the grid holds 27 x 3 x 4 x 5 = 1,620 scenarios.

The comparison between the models was measured using the absolute difference:

$$D = C_{BSG} - C_{BS} \quad (18)$$

where C_{BSG} is the Barles-Soner-GARCH price and C_{BS} is the Black-Scholes-GARCH benchmark price. The premium relative to the Black-Scholes benchmark is calculated as:

$$P_{BS} = \frac{C_{BSG} - C_{BS}}{C_{BS}} \times 100\% \quad (19)$$

Because the Black-Scholes benchmark price can be very small for out-of-the-money options with short maturities, the premium relative to the spot price is also reported:

$$P_{S_0} = \frac{C_{BSG} - C_{BS}}{S_0} \times 100\% \quad (20)$$

Reporting these two relative measures prevents interpretation from being dominated by scenarios where the benchmark option price is close to zero.

2.8 Solver Validation

The finite-difference solver is validated using a zero transaction cost threshold. When $\lambda = 0$, the correction in Equation (10) vanishes and Barles-Soner reduces to Black-Scholes on the same GARCH volatility, so the finite-difference prices should reproduce the analytical ones.

Validation used at-the-money one-year calls for all 27 stocks, a scenario sensitive to volatility and free of dominant intrinsic value. Absolute and relative errors between the finite-difference prices at $\lambda = 0$ and the analytical prices were computed, so that deviations at positive costs can be attributed to the nonlinear adjustment rather than to numerical artefacts. A paired Wilcoxon signed-rank test is also run between the two price sets at each positive cost level, chosen because the pairs share ticker, moneyness and maturity and no normality of differences is required.

2.9 Computational Implementation

The workflow of Figure 1 is implemented in Python: pandas for data management, statsmodels for the stationarity and ARCH tests, arch for GARCH estimation, numpy for computation and matplotlib for visualisation. Its outputs are the tables, diagnostics, price grids, validation results and figures reported below.

3. RESULT AND ANALYSIS

3.1 Verified LQ45 Sample and Return Characteristics

The final dataset holds the 27 stocks present in every official LQ45 announcement for the window. After cleaning, each has 937 corrected daily closing prices and 936 log returns from 2 February 2022 to 30 December 2025, with no missing values, so one pipeline applies uniformly.

Table 3. Summary of data structure and verified diagnostics

Item	Results	Note
Verified LQ45 stocks	27	Official constituents consistent
Price observations	937 per stock	2022-02-02 to 2025-12-30
Log return observations	936 per stock	First return undefined
Missing price values	0	Final panel processed
Stationary returns	27 of 27	ADF test at 5% level
Significant ARCH effect	26 of 27	ASII is the sole exception
Residual ARCH after GARCH	1 of 27	ADRO remains significant at 5%

Mean daily returns are close to zero while dispersion and tail behaviour differ markedly across stocks, the usual pattern in daily equity data. Table 4 reports the stocks with the largest dispersion or strongest tails in the verified sample.

Table 4. Descriptive statistics of selected daily LQ45 logarithmic returns

Stock	Mean	Std. Dev	Skewness	Kurtosis
BRPT	0.0014	0.0367	0.68	6.24
MDKA	-0.0005	0.0333	0.22	2.99
MEDC	0.0012	0.0309	0.63	3.17
INCO	0.0001	0.0285	0.43	2.77
ADRO	0.0009	0.0277	-0.36	15.96
PTBA	0.0006	0.0208	0.63	12.76
UNTR	0.0008	0.0206	-0.07	7.87
UNVR	-0.0003	0.0258	0.47	6.25

BRPT shows the largest return standard deviation in the selected group, while ADRO and PTBA carry the largest kurtosis, 15.96 and 12.76, indicating thick tails and extreme movements. These features support conditional rather than constant volatility modelling, consistent with the LQ45 volatility and GARCH option pricing literature [7], [10], [1]

3.2 Stationarity, ARCH Effect, and GARCH Diagnostics

The Augmented Dickey-Fuller test rejects a unit root for all 27 series at the 5% level, so the returns are suitable for volatility modelling, and the ARCH-LM test finds a significant ARCH effect in 26 of 27, confirming that variance is time-varying and justifying the GARCH family. ASII is the sole exception, with an ARCH-LM p-value of 0.46. It is retained because it is an official constituent and one pipeline is applied throughout, and the exception is reported rather than hidden.

After estimation the standardized residuals were retested with ARCH-LM. The effect disappears for 26 of 27 stocks. ADRO remains significant at the 5% level with a p-value of 0.03, so its forecast warrants more caution. This is acceptable for an aggregate experiment because the issue is confined to one stock, is reported explicitly, and affects a single input within a broad grid; retaining ADRO also keeps the empirical object fixed rather than trimming it on one diagnostic. To confirm the two weaker inputs do not drive the aggregate, the grid was resummarised with ADRO and ASII excluded. The mean premium relative to spot at a cost of 0.020 moves from 7.51% on the full panel to 7.54% on the reduced 25-stock panel, 0.03 percentage points, with smaller shifts at lower costs. The findings are therefore insensitive to the two weakest series.

3.3 GARCH Volatility Estimation Results

The model is estimated separately per series and the one-step-ahead forecasts are annualised as inputs to both pricing models. Table 5 reports the ten largest.

Table 5. Largest predicted annual GARCH volatility

Stock	α_1	β_1	Predicted Vol.	Post-estimation ARCH-LM p-value
INCO	0.0615	0.9347	0.7074	0.9256
BRPT	0.0600	0.9298	0.5221	0.7201
EXCL	0.0399	0.9580	0.5094	0.6820
MDKA	0.0477	0.9317	0.4812	0.1962
MEDC	0.0314	0.9340	0.4236	0.9374
ANTM	0.0526	0.9415	0.3942	0.8302
UNVR	0.0976	0.8554	0.3920	0.9906
KLBF	0.0473	0.9295	0.3727	0.6909
INKP	0.1032	0.8028	0.3715	0.6828
ADRO	0.1308	0.6578	0.3685	0.0332

INCO has the highest predicted annual volatility at 0.71, followed by BRPT at 0.52 and EXCL at 0.51; the panel mean is 0.33 and the minimum 0.14, so the verified constituents are far from a uniform volatility profile. This spread matters because volatility drives the time value of a call. Under Black-Scholes a higher input raises the price directly; under Barles-Soner the GARCH figure is the base volatility σ_0, which the nonlinear correction then adjusts. Volatility estimation is thus a pricing input, not a preliminary step.

3.4 Solver Validation at the Zero Transaction Cost Boundary

Before the positive-cost prices are interpreted, the solver is validated at the zero-cost boundary, where the correction vanishes and Barles-Soner collapses onto Black-Scholes, so the finite-difference and analytical prices should agree.

Table 6. Barles-Soner solver validation at zero transaction cost

Validation Metric	Value
Number of stocks tested	27
Mean absolute error	0.83
Maximum absolute error	4.34
Mean relative error	0.10%
Maximum relative error	0.23%

Table 6 shows small numerical errors, a mean relative error of 0.10% and a maximum of 0.23%, which supports the solver. Deviations at positive costs can therefore be read as nonlinear transaction cost adjustments rather than numerical artefacts, a check nonlinear models require because they lack closed-form solutions [19], [24], [20].

Because one mesh could flatter the solver, validation was repeated under refinement. Doubling the nodes to 360 cuts the mean relative error from 0.10% to 0.06% and the maximum from 0.23% to 0.08%, the monotone improvement a convergent scheme should show; doubling the domain to eight times the larger of spot and strike changes the mean error only in the fifth decimal, confirming the truncation boundary is far enough away; and doubling the time steps to 504 lowers it to 0.08%. Premiums move by under 0.20 percentage points for the five highest-premium stocks at a cost of 0.020 across all four configurations.

3.5 Black-Scholes-GARCH and Barles-Soner-GARCH Pricing Results

The experiment evaluates 1,620 scenarios from 27 stocks, three moneyness levels, four maturities and five cost levels. Table 7 summarises the comparison at each cost level.

Table 7. Summary of prices by proportional transaction cost

Transaction Cost	Mean Black-Scholes Price	Mean Barles-Soner Price	Mean Difference	Median Premium vs. BS	Mean Premium vs. Spot
0.000	496.93	496.93	0.00	0.00%	0.00%
0.005	496.93	691.92	195.00	34.03%	3.02%
0.010	496.93	803.59	306.67	55.15%	4.91%
0.015	496.93	867.64	370.71	72.17%	6.37%
0.020	496.93	908.81	411.89	87.88%	7.51%

At zero cost the two prices coincide by construction. As the cost rises the mean Barles-Soner-GARCH price increases monotonically, the mean difference growing from Rp195.00 at 0.005 to Rp411.89 at 0.020. The pattern follows the model structure: costs raise effective volatility, and higher effective volatility raises call premiums.

The paired Wilcoxon test returns an identical statistic of 52650 at every positive cost because all 324 pairs differ in the same direction. That is a foregone conclusion rather than evidence: the correction is non-negative by construction, so one-signed differences are guaranteed and the test cannot discriminate. Effect sizes and dispersion are reported instead of a p-value. Bootstrapping over 10,000 resamples gives a mean premium relative to spot of 3.02% with a 95% interval of 2.85% to 3.19% at a cost of 0.005, rising to 7.51% with an interval of 7.12% to 7.92% at 0.020. Dispersion across contracts far exceeds that sampling uncertainty: the tenth to ninetieth percentile range spans 1.22% to 5.06% of spot at 0.005 and 3.04% to 12.41% at 0.020, with a standardised effect size near 2.0 throughout. Contract design, not estimation noise, determines the premium a position attracts.

Table 8. Mean Barles-Soner premium relative to spot (%) under normal and Student-t innovations

Innovation law	Cost 0.005	Cost 0.010	Cost 0.015	Cost 0.020
Normal (baseline)	3.02	4.91	6.37	7.51
Student-t	3.11	5.06	6.57	7.76
Difference (pp)	0.10	0.15	0.20	0.25
Student-t mean price (Rp)	703.22	816.01	881.04	923.84

Table 8 makes the heavy-tail robustness check verifiable directly rather than through figures scattered in the text. The Akaike criterion prefers Student-t for all 27 stocks, by 26.1 to 188.4 units, with degrees of freedom from 3.02 to 7.40, and the heavier tails raise the annualised forecast for 23 of the 27 stocks by 5.06% on average. The premium is higher under Student-t at every positive cost level, so every normal-innovation figure here is a lower bound, and interpolated across the calibrated band of Table 10 the practically relevant premium moves from 1.51%-4.39% of spot to 1.56%-4.52%. The cross-section is unchanged: the same five leading stocks, with INKP and EXCL exchanging places, and the same dominant one-year 1.10-moneyness cell, at 11.98% of spot against 12.28%.

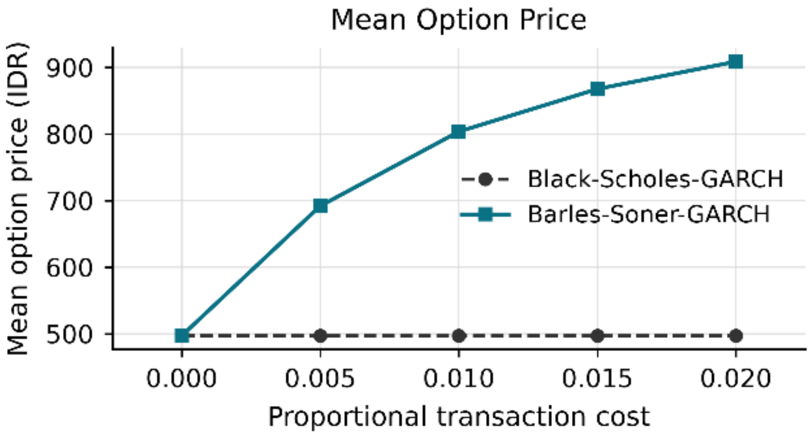

Figure 2. Mean option price in rupiah by proportional transaction cost

Because the premium relative to Black-Scholes explodes when the benchmark price is near zero, as it is for short-dated out-of-the-money calls, the premium relative to spot is also reported. Figure 3 shows it rising from 3.02% at a cost of 0.005 to 7.51% at 0.020, a more stable scale for economic interpretation.

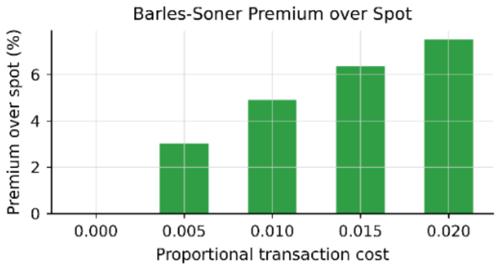

Figure 3. Mean Barles-Soner premium as a percentage of spot, by proportional transaction cost

3.6 The Effect of Moneyness, Maturity, and Stock-Level Volatility

The effect is not uniform across contracts. Figure 4 gives the mean premium relative to spot at the highest cost by moneyness and maturity, showing joint dependence on strike position and horizon.

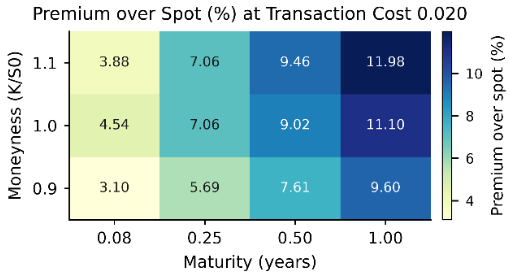

Figure 4. Premium (% of spot) by moneyness and maturity at a transaction cost of 0.020

The heatmap follows the structure of option pricing, but the two normalisations peak in different places and must be read separately. Against spot the premium rises in both dimensions to a maximum of 11.98% in the one-year 1.10-moneyness cell, with marginals climbing from 6.50% to 8.09% across moneyness and 3.84% to 10.89% across maturity. Against the Black-Scholes price the maturity ordering reverses and the maximum of 539% sits in the one-month 1.10-moneyness cell, because that benchmark is almost zero. Gamma is a third and distinct fact: largest near the money, which is why the at-the-money column exceeds the in-the-money column at every maturity. Premium relative to spot is this article's primary measure because the Black-Scholes ratio is unstable where the benchmark collapses.

Stock-level differences are equally clear. Figure 5 ranks the largest mean premiums relative to spot at the highest cost: INCO at 14.68%, INKP and EXCL at 11.15%, BRPT at 10.81% and UNTR at 9.94%. This tracks the GARCH output, since INCO, BRPT and EXCL carry the highest predicted volatilities. UNTR stands out not merely for its high spot price but because its premium stays large after normalisation across every moneyness and maturity, which shows the correction responds to the joint interaction of volatility, gamma, strike position and horizon.

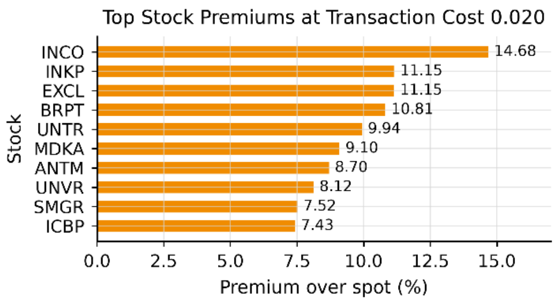

Figure 5. Stocks with the largest mean Barles-Soner premium, as a percentage of spot, at a transaction cost of 0.020

3.7 Risk-Aversion Sensitivity of the Transaction Cost Premium

Because the risk-aversion multiplier scales the transaction-cost term, every premium so far is conditional on normalising it to one. The whole grid was therefore recomputed at 0.5, 1, 2 and 5, holding sample, volatility inputs, solver settings and risk-free rate fixed, giving 6,480 prices. Reproduction at the baseline is exact, every price recovered to a maximum absolute deviation of zero, so the sweep is directly comparable with Table 7. Table 9 reports the mean premium relative to spot.

Table 9. Mean Barles-Soner premium relative to spot (%) by risk-aversion multiplier

Risk Aversion	Cost 0.005	Cost 0.010	Cost 0.015	Cost 0.020
0.5	2.35	3.86	5.11	6.14
1 (baseline)	3.02	4.91	6.37	7.51
2	3.86	6.14	7.74	8.80
5	5.29	7.95	9.34	10.03

Three results follow. First, the premium increases in risk aversion at every cost level, which is the expected direction, but far less than proportionally. A tenfold increase, from 0.5 to 5, lifts the mean premium at a cost of 0.020 only from 6.14% to 10.03% of spot, about 63%. The estimated elasticity falls from 0.35 at a cost of 0.005 to 0.21 at 0.020, close to the cube-root behaviour implied by the asymptotic form of the correction at small arguments rather than the linear scaling the squared-cost term alone suggests. The concavity of the correction therefore damps the influence of the risk-aversion assumption substantially.

Second, the sweep confirms numerically that the cost parameter and the multiplier enter only through their product. A cost of 0.005 at a multiplier of 2 and a cost of 0.010 at 0.5 both return 3.86% of spot, and 0.010 at 2 matches 0.020 at 0.5 at 6.14%, with a maximum deviation of zero across matched scenarios. The two are therefore not separately identified: doubling assumed risk aversion is observationally equivalent to scaling the cost by the square root of two, so the reported grid can be reinterpreted for any alternative assumption without re-solving.

Third, the qualitative conclusions hold. The premium stays non-negative and monotone in cost for every stock, moneyness, maturity and multiplier. The largest premium relative to spot is the one-year out-of-the-money cell at all four multipliers and INCO leads throughout; only the composition of the leading group shifts at the top, MDKA and ANTM displacing UNTR and INKP at a multiplier of 5 as the correction saturates. The reading advanced here therefore does not rest on the baseline normalisation.

3.8 Calibration of the Transaction Cost Parameter to Observable IDX Cost Levels

The premiums above are indexed to a cost grid chosen as a controlled range rather than measured, which leaves open whether it spans plausible Indonesian values. This subsection anchors it by decomposing the round-trip cost of trading LQ45 equities into explicit and implicit components, both measurable from broker tariffs and equity data.

The explicit component comes from a published Indonesian brokerage schedule [31]: online commissions of about 0.15% on purchases and 0.25% on sales, inclusive of the exchange, clearing and depository charges brokers pass through, plus a 0.1% final income tax on the gross value of sales only. A buy-then-sell cycle therefore costs roughly 0.50%, or 0.25% per leg. These are contractual and need no estimation, and no separate exchange fee is added because the pass-through is already embedded, which avoids double counting. Since one non-peer-reviewed tariff should not carry the floor alone, the band is also computed under discount rates of 0.10% and 0.20% and full-service rates of 0.20% and 0.30%; these move the one-way explicit cost only between 0.20% and 0.30%.

The implicit component, the effective bid-ask spread, is not directly observable but can be inferred. Trading costs induce negative first-order serial dependence in observed price changes, and Roll [32] shows the effective spread is then twice the square root of the negative of that covariance. Applied to the 936 daily returns of each constituent, the estimator is defined for 20 of 27 stocks; for ANTM, BBNI, BBTN, BRPT, INCO, MDKA and SMGR the sample covariance is positive and no real solution exists, a known failure mode reported here rather than repaired by sign reversal. Across the 20 defined cases the spread has a median of 1.22% of price and ranges from 0.31% for BMRI to 2.11% for ADRO, a median half-spread of 0.61% per leg.

That figure is an upper bound, not a point estimate. Harris [33] shows the serial-covariance estimator is biased upward in finite samples and unreliable when its assumptions fail, and the seven undefined cases are direct evidence of such failure here. Daily closing prices compound the problem, since any negative dependence from short-horizon reversal is attributed to the spread.

The calibration is therefore a band. Its floor is the contractual explicit cost, incurred on every transaction regardless of liquidity; its ceiling adds the median Roll half-spread, generous for the reason just given. One check bears on whether the surviving subsample biases that median upward, which it would if the seven undefined names were the most liquid. The comparison points the other way: the undefined group has significantly higher GARCH volatility, medians of 0.394 against 0.269 with a Mann-Whitney p-value of 0.016, while spot prices do not differ at $p = 0.533$. Since spreads rise with volatility, excluding the more volatile names depresses rather than inflates the median, so the ceiling is if anything understated. Table 10 reports the decomposition.

Table 10. Decomposition of LQ45 round-trip transaction costs and the implied calibration band

Cost component	Percent of value	As transaction cost
Buy commission, reference schedule	0.150	0.00150
Sell commission, reference schedule	0.250	0.00250
Final income tax, sales only	0.100	0.00100
Round-trip explicit cost	0.500	0.00500
One-way explicit cost	0.250	0.00250
Roll half-spread, range across stocks	0.153–1.057	0.00153–0.01057
Roll half-spread, median stock	0.612	0.00612
Calibrated one-way cost, lower end (explicit only)	0.250	0.00250
Calibrated one-way cost, upper end (with Roll)	0.862	0.00862

The observable one-way cost lies between 0.00250 and 0.00862 in grid units, with three consequences. The lowest positive grid point, 0.005, falls inside this band, so its premium of 3.02% of spot is closest to what an Indonesian participant faces. Interpolating across the band gives 1.51% of spot at the floor and 4.39% at the ceiling — the range this article defends as its empirical claim. The highest grid point, 0.020, exceeds the ceiling by a factor of 2.3 and the floor by 8, so its 7.51% is a stress scenario reached only under severe illiquidity or rebalancing far more frequent than the daily discretisation assumed here. Widening the explicit component to discount and full-service schedules shifts the band only to 0.00200–0.00912.The empirical contribution is thus applying the nonlinear framework to a verified multi-stock LQ45 sample rather than one illustrative stock, and quantifying the premium against a validated frictionless comparator. Relative to [19] and [20], the distinction is specific and limited: those studies solve the same model correctly, and the difference lies in the empirical object and its verification — a constituent-verified panel, GARCH rather than assumed volatility, and a premium validated at the zero-cost boundary, checked under refinement and calibrated to measured costs. No claim of superior modelling is intended.

4. CONCLUSION

This study developed and validated a Barles-Soner-GARCH framework for pricing European calls on constituent-verified LQ45 stocks. Across the 27-stock panel all return series are stationary and 26 show a significant ARCH effect, supporting conditional rather than constant volatility. Two exceptions are carried forward rather than smoothed over: ASII shows no significant ARCH effect before estimation and ADRO retains one afterwards, so their volatility inputs are the least reliable in the panel.

The solver is consistent at the zero-cost boundary, with a mean relative error of 0.10%, so differences at positive costs follow from the nonlinear correction rather than numerical artefacts. Barles-Soner-GARCH prices exceed Black-Scholes-GARCH throughout, the mean premium relative to spot rising from 3.02% at a cost of 0.005 to 7.51% at 0.020. That range is not the practical premium: calibration to observable Indonesian costs places the representative one-way cost between 0.00250 and 0.00862, a premium near 1.51% to 4.39% of spot, while 7.51% belongs to a stress scenario 2.3 to 8 times prevailing costs and is mildly cap-limited. Because the sign is structural, significance testing is uninformative and bootstrap intervals are reported instead, 2.85% to 3.19% of spot at a cost of 0.005. The premium varies by contract: against spot it rises in both moneyness and maturity, peaking at 11.98% in the one-year 1.10-moneyness cell, while gamma is largest near the money, which is why the at-the-money column exceeds the in-the-money column at every maturity. The leading stocks are INCO, INKP, EXCL, BRPT and UNTR, predominantly high-volatility names, so the premium reflects conditional volatility, gamma, strike position and horizon jointly rather than volatility alone.

The contribution is empirical scope and methodological rigour rather than model novelty: a constituent-verified LQ45 panel, stock-level GARCH(1,1) volatility, a solver validated at the zero-cost boundary and under refinement, and effect sizes with bootstrap intervals across 1,620 scenarios in one framework. Against [19] and [20], which illustrate a single underlying, this extends Barles-Soner pricing to a broader verified Indonesian sample. The direction of the effect is structural; what is new is its measured magnitude and cross-sectional pattern.

A risk-aversion sweep supports these conclusions. Recomputing at multipliers of 0.5, 1, 2 and 5 raises the mean premium (cost = 0.020) from 6.14% to 10.03% of spot — an elasticity well below one — and shows that cost and multiplier are identified only through their product, so the grid can be reinterpreted for any alternative assumption without re-solving. Sign, monotonicity, dominant cell, and leading stock hold across all four settings, and excluding the two weakest series shifts the aggregate premium by at most 0.03 percentage points. Three scope limitations remain: only European calls are covered; conditional variance uses GARCH(1,1) with normal innovations as the baseline — rejected by the Akaike criterion for all 27 stocks in favor of Student-t, but retained for yielding the more conservative premium, with the Student-t grid in Table 8; and the risk-free rate is held constant. The cost calibration is a band, its explicit component following a published schedule and its implicit component carrying the Roll estimator's upward bias. Natural extensions include asymmetric and heavy-tailed specifications, intraday microstructure data for calibration, and comparison with traded premiums once a liquid Indonesian option or warrant series exists.

5. REFERENCES

[1] R. M. Ponziani, "The Modeling the Returns Volatility of Indonesian Stock Indices: The Case of SRI-KEHATI and LQ45," *Jurnal Ekonomi Modernisasi*, vol. 18, no. 1, pp. 13–21, 2022, https://doi.org/10.21067/jem.v18i1.6411.

[2] F. Black and M. Scholes, "The Pricing of Options and Corporate Liabilities," *Journal of Political Economy*, vol. 81, no. 3, pp. 637–654, 1973, https://doi.org/10.1086/260062.

[3] R. C. Merton, "Theory of Rational Option Pricing," *The Bell Journal of Economics and Management Science*, vol. 4, no. 1, pp. 141–183, 1973, https://doi.org/10.2307/3003143.

[4] J.-P. Chavas, J. Li, and L. Wang, "Option Pricing Revisited: The Role of Price Volatility and Dynamics," *Journal of Commodity Markets*, vol. 33, 2024, https://doi.org/10.1016/j.jcomm.2023.100381.

[5] X.-J. He and S. Lin, "A Fractional Black-Scholes Model with Stochastic Volatility and European Option Pricing," *Expert Syst. Appl.*, vol. 178, 2021, https://doi.org/10.1016/j.eswa.2021.114983.

[6] T. Wang, S. Cheng, F. Yin, and M. Yu, "Overnight Volatility, Realized Volatility, and Option Pricing," *Journal of Futures Markets*, vol. 42, no. 7, pp. 1264–1283, 2022, https://doi.org/10.1002/fut.22330.

[7] M. Escobar-Anel, J. Rastegari, and L. Stentoft, "Option Pricing with Conditional GARCH Models," *Eur. J. Oper. Res.*, vol. 289, no. 1, pp. 350–363, 2021, https://doi.org/10.1016/j.ejor.2020.07.002.

[8] D. H. Oh and Y.-H. Park, "GARCH Option Pricing with Volatility Derivatives," *J. Bank. Financ.*, vol. 146, 2023, https://doi.org/10.1016/j.jbankfin.2022.106718.

[9] Z. Fang and J.-Y. Han, "Realized GARCH Model in Volatility Forecasting and Option Pricing," *Comput. Econ.*, vol. 66, no. 5, pp. 3637–3657, 2025, https://doi.org/10.1007/s10614-024-10826-8.

[10] M. Escobar-Anel, L. Stentoft, and X. Ye, "The Benefits of Returns and Options in the Estimation of GARCH Models: A Heston-Nandi GARCH Insight," *Econom. Stat.*, vol. 36, pp. 1–18, 2025, https://doi.org/10.1016/j.ecosta.2022.12.001.

[11] M. Escobar-Anel, L. Stentoft, and X. Ye, "Not All VIXs Are (Informationally) Equal: Evidence from Affine GARCH Option Pricing Models," *Financ. Res. Lett.*, vol. 69, 2024, doi: 10.1016/j.frl.2024.106053.

[12] C. Chorro and R. H. Fanirisoa Zazaravaka, "Discriminating Between GARCH Models for Option Pricing by Their Ability to Compute Accurate VIX Measures," *Journal of Financial Econometrics*, vol. 20, no. 5, pp. 902–941, 2022, https://doi.org/10.1093/jjfinec/nbaa042.

[13] N. Zulfiqar and S. Gulzar, "Implied Volatility Estimation of Bitcoin Options and the Stylized Facts of Option Pricing," *Financial Innovation*, vol. 7, no. 1, 2021, https://doi.org/10.1186/s40854-021-00280-y.

[14] T. Pang and Y. Zhao, "On GARCH and Autoregressive Stochastic Volatility Approaches for Market Calibration and Option Pricing," *Risks*, vol. 13, no. 2, 2025, https://doi.org/10.3390/risks13020031.

[15] P. J. Venter and E. Mare, "GARCH Option Pricing and Implied FX Volatility Indices," *Studies in Economics and Econometrics*, vol. 45, no. 1, pp. 42–52, 2021, https://doi.org/10.1080/03796205.2021.1956170.

[16] P. J. Venter and E. Mare, "Univariate and Multivariate GARCH Models Applied to Bitcoin Futures Option Pricing," *Journal of Risk and Financial Management*, vol. 14, no. 6, 2021, https://doi.org/10.3390/jrfm14060261.

[17] G. Barles and H. M. Soner, "Option Pricing with Transaction Costs and a Nonlinear Black-Scholes Equation," *Finance and Stochastics*, vol. 2, no. 4, pp. 369–397, 1998, doi: 10.1007/s007800050046.

[18] H. E. Leland, "Option Pricing and Replication with Transactions Costs," *J. Finance*, vol. 40, no. 5, pp. 1283–1301, 1985, https://doi.org/10.1111/j.1540-6261.1985.tb02383.x.

[19] D. M. F. Noor and R. Artiono, "Numerical Pricing of European Options under Proportional Transaction Costs: A Semi-Discretization Approach to the Nonlinear Barles-Soner Model," *ZERO: Jurnal Sains, Matematika dan Terapan*, vol. 10, no. 1, 2026, https://doi.org/10.30829/zero.v10i1.28084.

[20] M. Taufik and R. Artiono, "The Valuation of European Options with Transaction Costs Using the Barles-Soner Model," *ZERO: Jurnal Sains, Matematika dan Terapan*, vol. 9, no. 3, 2025, https://doi.org/10.30829/zero.v9i3.27702.

[21] R. Company, L. Jódar, and J.-R. Pintos, "Consistent Stable Difference Schemes for Nonlinear Black-Scholes Equations Modelling Option Pricing with Transaction Costs," *ESAIM: Mathematical Modelling and Numerical Analysis*, vol. 43, no. 6, pp. 1045–1061, 2009, https://doi.org/10.1051/m2an/2009014.

[22] J. de Frutos and V. Gatón, "A Pseudospectral Method for Option Pricing with Transaction Costs under Exponential Utility," *J. Comput. Appl. Math.*, vol. 394, 2021, https://doi.org/10.1016/j.cam.2021.113541.

[23] P. Pálvóra and D. Ševčovič, "Utility Indifference Option Pricing Model with a Non-Constant Risk-Aversion under Transaction Costs and Its Numerical Approximation," *Journal of Risk and Financial Management*, vol. 14, no. 9, 2021, https://doi.org/10.3390/jrfm14090399.

[24] M. Rezaei, A. R. Yazdanian, A. Ashrafi, and S. M. Mahmoudi, "Numerically Pricing Nonlinear Time-Fractional Black-Scholes Equation with Time-Dependent Parameters Under Transaction Costs," *Comput. Econ.*, vol. 60, no. 1, pp. 243–280, 2021, https://doi.org/10.1007/s10614-021-10148-z.

[25] T. Saeed, J. Hussain, and S. Rafique, "Option Pricing under Stochastic Interest Rates and Transaction Costs Using Physics-Informed Neural Networks," *Examples and Counterexamples*, vol. 10, 2026, https://doi.org/10.1016/j.exco.2026.100227.
[26] M. R. Shakeel, S. Yadav, and M. Ahmad, "Option Pricing under Regime-Switching Jump-Diffusion Dynamics with Transaction Costs: A Neural SDE Approach," *Review of Derivatives Research*, vol. 29, no. 1, 2026, https://doi.org/10.1007/s11147-026-09238-7.
[27] D. Yan, "A Comprehensive Study of Option Pricing with Transaction Costs," *Bull. Aust. Math. Soc.*, vol. 106, no. 3, pp. 522–524, 2022, https://doi.org/10.1017/S0004972722000740.
[28] X. Cai and Y. Wang, "A Novel Fourth-Order Finite Difference Scheme for European Option Pricing in the Time-Fractional Black-Scholes Model," *Mathematics*, vol. 12, no. 21, 2024, https://doi.org/10.3390/math12213343.
[29] Y. Feng, X. Zhang, Y. Chen, and L. Wei, "A Compact Finite Difference Scheme for Solving Fractional Black-Scholes Option Pricing Model," *J. Inequal. Appl.*, vol. 2025, no. 1, 2025, https://doi.org/10.1186/s13660-025-03261-2.
[30] P. Roul and V. M. K. P. Goura, "A Compact Finite Difference Scheme for Fractional Black-Scholes Option Pricing Model," *Applied Numerical Mathematics*, vol. 166, pp. 40–60, 2021, https://doi.org/10.1016/j.apnum.2021.03.017.
[31] B. R. I. D. Sekuritas, "Memahami Biaya Transaksi Saham Sebelum Mulai Investasi," 2025.
[32] R. Roll, "A Simple Implicit Measure of the Effective Bid-Ask Spread in an Efficient Market," *J. Finance*, vol. 39, no. 4, pp. 1127–1139, 1984, https://doi.org/10.1111/j.1540-6261.1984.tb03897.x.
[33] L. Harris, "Statistical Properties of the Roll Serial Covariance Bid/Ask Spread Estimator," *J. Finance*, vol. 45, no. 2, pp. 579–590, 1990, https://doi.org/10.1111/j.1540-6261.1990.tb03704.x.